DOI: 10.1002/chem.201001605

Formation of Metal-Assisted Stable Double Helices in Dimers of Cyclic Bis-Tetrapyrroles that Exhibit Spring-Like Motion

Takashi Hashimoto,[a] Takuma Nishimura,[a] Jong Min Lim,[b] Dongho Kim,[b] and Hiromitsu Maeda*[a, c]

Abstract: Bidipyrrin-bridged macrocycles, prepared from Ni^{II}-bridged dipyrrin-based nanorings by intramolecular oxidative biaryl coupling reactions, yielded [2+4]-type Zn^{II}-assisted stable twisted-ring dimers comprising two double helices. These [2+4]-type metal complexes can be optically resolved by chiral HPLC and exhibit tunable electronic and optical properties as a result of spring-like motions. The double helices behave as glue to connect two macrocycles and as the screws of hinges to form thermally responsive synchronized spring systems.

Keywords: chirality · coordination compounds · heterocycles · macrocycles · self-assembly

Introduction

The control of chirality in metal-assisted assemblies[1] is an important issue in the production of promising catalysts for asymmetric synthesis.[2] In addition, chirality-amplified macromolecular systems have attracted considerable attention since Lee and co-workers reported the temperature-dependent conformational changes in the single helical springs of coordination polymers.[3] As small discrete systems,[4] Th^{IV}-assisted quadruple-stranded bis-bidentate helicates were found by Xu and Raymond[5] and self-organized Cu^{I}-bridged double helices were developed by Nitschke and co-workers using nitrogen-containing aromatic ligands.[6] In many cases the chirality in metal–ligand clusters can be controlled by auxiliaries such as the chiral substituents of ligand molecules. On the other hand, metal coordination itself affords racemic forms of chiral assemblies based on achiral ligands. In most cases the optical resolution of such racemic mixtures, which would provide various valuable chiral clusters, is not easy to achieve,[7] especially in the case of metal-assisted helices, because of fairly weak metal–ligand interactions.

As potential building subunits of helical assemblies, linear tetrapyrrole ligands, bidipyrrins, that is, directly linked dipyrrin dimers,[8,9] can be used to fabricate metal complexes, including [2+2]-type Zn^{II}-assisted double helices[10] as well as roughly square-planar complexes formed with Ni^{II}, Cu^{II}, and Pd^{II}[11] (Scheme 1). Because of the coordination properties of dipyrrins as monoanionic bidentate ligands, bidipyrrin–Zn^{II} double helices are electronically neutral and therefore their enantiomers would be isolated from the racemic mixture by facile protocols such as chiral HPLC. However,

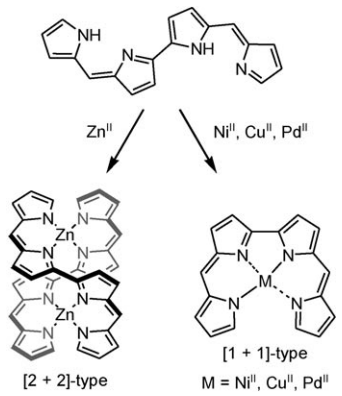

Scheme 1. Metal coordination modes of bidipyrrin as the parent structure.

[a] T. Hashimoto, T. Nishimura, Prof. Dr. H. Maeda
College of Pharmaceutical Sciences
Institute of Science and Engineering
Ritsumeikan University, Kusatsu 525-8577 (Japan)
Fax: (+81) 77-561-2659
E-mail: maedahir@ph.ritsumei.ac.jp

[b] J. M. Lim, Prof. Dr. D. Kim
Department of Chemistry, Yonsei University
Seoul 120-749 (Korea)

[c] Prof. Dr. H. Maeda
PRESTO, Japan Science and Technology Agency (JST)
Kawaguchi 332-0012 (Japan)

Supporting information for this article is available on the WWW under http://dx.doi.org/10.1002/chem.201001605.

there have been no reports of optically resolved bidipyrrin-based double helices presumably due to their fragility even though they are constructed of electronically compensating N–Zn bonds. Stimulated by the fascinating but almost unexplored properties of bidipyrrins, we have investigated the formation, topological control, and properties of these optically resolved and stable helical structures.

Results and Discussion

Properties of Zn^{II}-assisted double helices based on *meso*-arylbidipyrrin derivatives: Initially we attempted to reveal the detailed properties of Zn^{II}-coordinated bidipyrrin-based double helices. To explore the possibility of their optical resolution and to examine their stabilities as pure enantiomers in various solvents, the double-helical Zn^{II} complexes (**1a–d**) of *meso*-arylbidipyrrins, including hexadecyloxy- and triethyleneglycol (TEG)-substituted derivatives, were prepared by an oxidative biaryl coupling reaction of Ni^{II} complexes of the corresponding dipyrrins and subsequent demetalation and Zn^{II} complexation (Figure 1a). The double helices **1a–d** can be optically resolved by chiral HPLC (Daicel IA, hexane/CH_2Cl_2/Et_2NH = 95:5:0.5 for **1a**,**b**, hexane/CH_2Cl_2 = 7:1 for **1c**, and hexane/THF/Et_2NH = 50:50:0.1 for **1d**). In solution, the optically pure double helices **1a–d**, which show CD signals after resolution, were transformed into mixtures

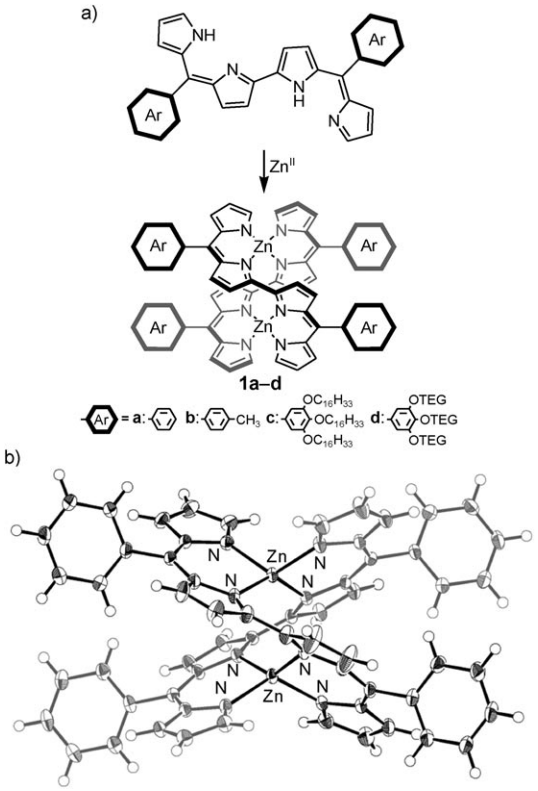

Figure 1. a) Zn^{II} coordination of *meso*-arylbidipyrrin derivatives and b) the ORTEP drawing (ellipsoids drawn at the 50% probability level) of the single-crystal X-ray structure of **1a** (*M* type, front view).

of enantiomers under specific conditions. For example, **1a–c** show a slow transition between enantiomers in $CHCl_3$ at room temperature, presumably due to the existence of a trace amount of electron-pair donor species as well as the electron-pair donating nature of $CHCl_3$ itself. The transitions occur over several hours and so temporary optical resolutions were performed. However, it is difficult to establish fixed conditions using $CHCl_3$ and to estimate exact kinetic parameters for the racemization processes. The fragility of a single lock was also suggested by the ligand-exchange behavior of **1a** and **1b** in $CHCl_3$ in which the ligand-exchanged mass of these double helices was observed. In THF, **1a–c** maintain their enantiomeric purities at room temperature but exhibit a slow transition to the racemic state at 60 °C, possibly due to the electron-pair donating nature of THF that is suitable for metal coordination. In THF at 60 °C, no ligand exchange between bidipyrrin–Zn^{II} complexes were observed. Therefore the racemization can be considered to occur through a first-order reaction: The kinetic parameters (k) of the racemization of **1a**,**c** at 60 °C were estimated to be 4×10^{-5} and 9×10^{-6} s^{-1}, respectively, which are possibly dependent on the electron-donating aryl substituents and are correlated with the metal-coordination ability of the pyrrole nitrogen atom. Furthermore, aliphatic **1c**, which is soluble in hydrocarbon solvents as a monomer according to its UV/Vis absorption spectrum, does not show diminished CD signals in hexane even at 60 °C because of the very weak coordination properties of the solvent. On the other hand, amphiphilic **1d**, which is soluble in water and forms aggregates mainly on the scale of 180 and 330 nm at 20 and 80 °C, respectively, as observed by dynamic light-scattering (DLS) measurements, shows racemization behavior in aqueous solution at 90 °C. Apart from inert solvents such as hexane, Zn^{II}-assisted bidipyrrin double helices show transitions between enantiomers in various solvents, at least at high temperatures. Although further investigations should be made, including the determination of intermediates or transition states during racemization, the fragility of bidipyrrin-based double helices was demonstrated.

The double helical structure of *meso*-phenyl **1a** was revealed by single-crystal X-ray analysis (Figure 1b), which showed the absence of significant interactions between π-conjugated moieties in the solid state.[12] Single-crystal analysis of **1a** revealed temperature-dependent behavior in the double helical structure with Zn^{II}–Zn^{II} distances of 3.243 and 3.254 Å at 123 and 297 K, respectively. This observation, the reduced heights of the double helix and the extended widths at 123 K compared with those a 297 K, suggests that the bidipyrrin-based double helices can be useful building blocks of stimuli-responsive chiral systems not only in the solid state but also in solution, which would enable more dynamic spring-like motions. In fact, the double helix of **1a** exhibits significant changes in its ^1H NMR and UV/Vis absorption spectra as the temperature varies: from 60 to −60 °C, the resonance of, for example, the pyrrole α-CH at 7.22 ppm is shifted upfield to 7.01 ppm in $CDCl_3$ and the absorbance at λ_{max} = 572 nm increased by around 1.9-fold in $CHCl_3$ as a

result of the flexibility of the double helix. However, it is not easy to discuss the detailed temperature-dependent helical motions by CD spectral changes because of racemization in this solvent.

Synthesis and characterization of bidipyrrin-based macrocycles and metal complexes: One of the effective strategies for forming stable bidipyrrin double helices is the coordination of multiple (more than two) Zn^{II} ions. As candidate ligand molecules for such multinuclear complexes, covalently linked cyclic bis-bidipyrrins (cBDPR, **4a**,**b**) were obtained as dark-blue solids in yields of 78 and 48% (two steps) by a biaryl coupling of Ni^{II} nanorings (*mmm*-DPR_2Ni_2, **2a**,**b**)[13] and subsequent demetalation of **3a**,**b** (Scheme 2). In contrast to **2a**,**b**, which exhibit temperature-dependent paramagnetic ^{1}H NMR shifts because of the distortion of the square-planar coordination, **3a**,**b** show diamagnetic features due to the approximate square-planar coordination of Ni^{II}. By treating **4a** with $Ni(OAc)_2$ and $Cu(OAc)_2$ (10 equiv in each) in $CHCl_3$ and stirring the resultant solution at room temperature for 5 h, we obtained brown and red solids of [1+2]-type Ni^{II} and Cu^{II} complexes **3a** and **3′a** in yields of 91 and 40%, respectively. In sharp contrast, the treatment of **4a**,**b** with $Zn(OAc)_2$ (10 equiv) for 5 h in $CHCl_3$ resulted in the formation of Zn^{II}-bridged [2+4]-type dimers **5a**,**b**, as revealed by ^{1}H NMR spectroscopy (see below) and MALDI-TOF MS, as green solids in yields of 71 and 60%, respectively. Similarly, treatment with $Cd(OAc)_2$ under appropriate conditions also resulted in the formation of the MALDI-TOF MS peak of the [2+4]-type complex. The addition of 1.0 equiv of $Zn(OAc)_2$ to **4a** led to the formation of complicated mixtures, including intermediate complexes such as [2+2]- and [2+3]-type complexes, as a result of a small amount of metal cations for [2+4]-type complexation. No ligand exchange was observed for **5a** and **5b** on heating at reflux in $CHCl_3$ and toluene, whereas the addition of acids such as aq. HCl readily led to the demetalation of **5a** to give **4a**. The UV/Vis absorption spectra of **4a**, protonated **4a**, **3a**, **3′a**, and **5a** in $CHCl_3$ were quite distinct with absorption maxima (λ_{max}) at 410, 587, and 724 nm for **4a**, 440 and 691 nm for protonated **4a**, 412, 575, and 845 nm for **3a**, 467, 575, and 769 nm for **3′a**, and 424 and 655 nm (br) for **5a** (Figure 2). Fluorescence emission of **5a** in $CHCl_3$ was observed at 822 nm ($\lambda_{ex}=655$ nm, $\Phi_F=0.006$). The electronic nature of **5b** is very similar to that of **5a**, as illustrated by the λ_{max} at 425 and 651 nm (br) and the λ_{em} at 822 nm ($\lambda_{ex}=$ 651 nm, $\Phi_F=0.006$) in $CHCl_3$.

The ^{1}H NMR spectrum of **5a** in [D_8]THF exhibited 22 unique peaks arising from the helical structure formed on Zn^{II} complexation in the absence of diastereomers (Figure 3a). Furthermore, from the DOSY analysis of **3a**, **4a**,

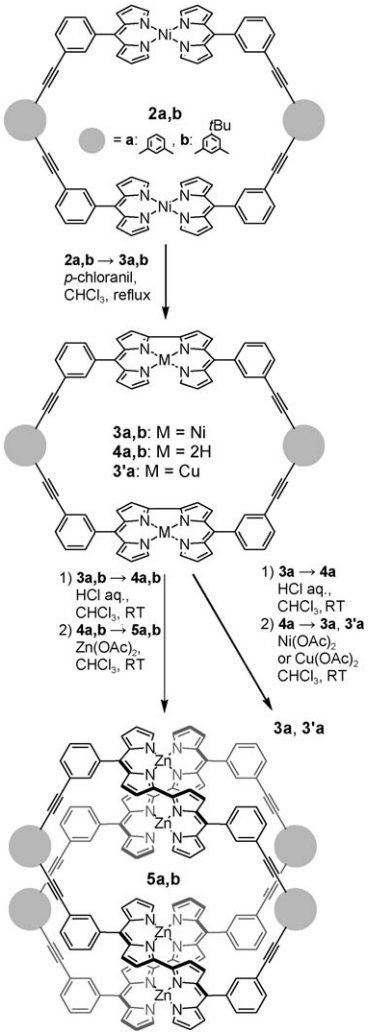

Scheme 2. Formation of metal complexes of bidipyrrin-based macrocycles.

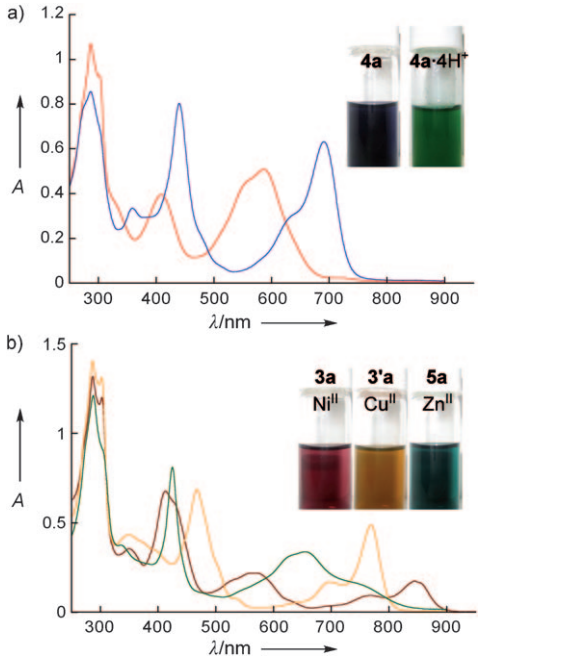

Figure 2. UV/Vis absorption spectra and colors (inset) in $CHCl_3$ of a) **4a** (red) and protonated **4a** (blue) and b) **3a** (brown), **3′a** (yellow), and **5a** (green).

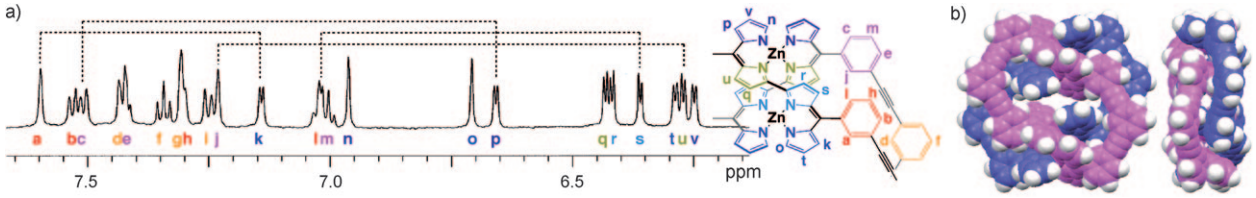

Figure 3. a) ^{1}H NMR spectrum of **5a** in [D$_8$]THF (600 MHz, 60 °C) with the correlations suggested by ^{1}H–^{1}H ROESY experiments and b) optimized structure of **5a** (*M* type) at the DFT level of theory.

and **5a** we observed that these complexes have diffusion coefficients of 5.1×10^{-10}, 6.8×10^{-10}, and 3.8×10^{-10} m^{2}s^{-1}, respectively. These values reflect the different sizes of these complexes. The structural optimization of **5a** at the B3LYP/6-31G** level of theory[14] supports the formation of [2+4]-type structures (Figure 3b). The dihedral angles between the dipyrrin moieties are 65.5–65.8°, whereas the Zn^{II}–Zn^{II} distances in the double helices and across the inner pore are 3.59 and 7.61 Å, respectively. Furthermore, the neighboring phenylethynyl spacers are quite strained with a dihedral angle of 35.4°. With the assistance of the optimized structure, all the proton signals were assigned on the basis of ^{1}H–^{1}H COSY and ROESY experiments, which showed correlations between the pyrrole β-CH and phenyl *o*-CH at the *meso* position. The variable-temperature (VT) NMR spectra of **5a** in [D$_8$]THF in the range of −60 to +60 °C showed temperature-dependent upfield shifts in many of the protons along with downfield shifts ($\Delta\delta=0.057$, 0.052, 0.008, 0.022, and 0.016 ppm) in the protons assigned to the *meso*-aryl-H (H^j and H^l), external pyrrole α-CH (H^n), and inner "bipyrrole" units (H^s and H^u). In particular, the chemical shifts of the external pyrrole-CH of **5a** (H^n, H^p, and H^v) exhibited behavior similar to that of the pyrrole-CH of **1a** (Figure 1b). Chemical shift changes in **1a** are larger than those in **5a**, which suggests that in solution the double helix of **1a** is more flexible than that of **5a**. Furthermore, XAFS revealed that the distances between two neighboring Zn^{II} in **1a** and **5a** are 3.17 and 3.24 Å, respectively, in a matrix of 2-methyl-THF at −163 °C, which suggests the formation of double helices.

In contrast to **1a–d**, the interlocked complexes **5a**,**b** retained their enantiopurity after optical resolution by chiral HPLC (Daicel IA, hexane/CHCl$_3$/Et$_2$NH = 80:20:0.1). This suggests that unstable double helices of bidipyrrin could be stabilized by dual locks, as observed in the case of **5a**,**b**. The enantiomers of **5a** in 2-methyl-THF exhibited Cotton effects in the CD spectra with λ_{max} at 336, 424, 618, 664, and 772 nm. The VT CD spectral changes of each enantiomer of **5a**,**b** in 2-methyl-THF revealed stronger Cotton effects at low temperatures because of a possible fastening of the pitches of the Zn^{II}-bridged double helices as springs (Figure 4a). These changes correlated well with the corresponding UV/Vis absorption (Figure 4b) and fluorescence spectral changes. Such temperature-dependent spectral changes of **5a**,**b** were also observed in CHCl$_3$, THF, and toluene. In 2-methyl-THF, **5a**,**b** shows similar UV/Vis and CD spectral

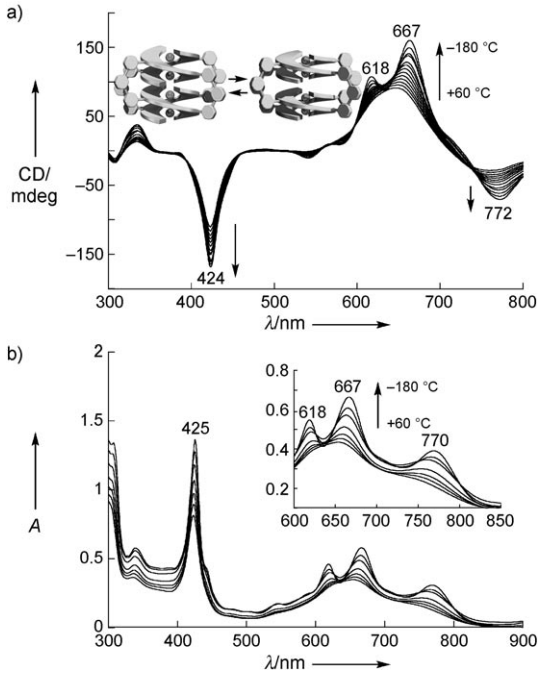

Figure 4. a) VT CD spectra of **5a** in 2-methyl-THF (2.8×10^{-6} M at RT) and possible conformational changes (inset) and b) the corresponding VT UV/Vis absorption spectra.

changes, even below the glass transition temperature (T_g), to those in solution, whereas the fluorescence emissions are significantly enhanced below the T_g. Furthermore, the smaller dihedral angles at the bipyrrole units, which indicate the fastening of helical pitches, should provide enhanced absorption bands at low temperatures. The temperature-dependent changes in the helical pitches are consistent with the changes observed in the solid-state structures of **1a**, as discussed above. The CD changes that are dependent on the states of the helical pitches contrast those observed for equilibria between helical diastereomers or folding–unfolding oligomers.[15,16] To the best of our knowledge, this is the first example of temperature-dependent spring-like motions of metal complexes in which the enantiomeric purity of the helices is retained.

Photophysical properties tunable by external stimuli: The fluorescence lifetimes of **5a** in 2-methyl-THF at different temperatures were estimated from time-correlated single-photon counting (TCSPC) measurements. In the case of

metal-free **4a**, fluorescence dynamics revealed a single decay component of 0.48 ns at 24 °C and an increased decay component at low temperatures (1.9 ns at −196 °C). In contrast, at high temperatures, **5a** exhibited two decay components (0.040 and 0.60 ns at 24 °C) whereas at low temperatures the fast decay component of **5a** disappeared with the lifetime of the second component increasing (3.0 ns at −196 °C). This indicates that **5a** has a second relaxation pathway from the excited to the ground state that is absent in **4a**. Note also that this relaxation pathway is blocked at low temperatures. From these observations it can be concluded that the fast decay component of **5a** is a result of the flexible spring-like motion, which can be controlled by external stimuli.

Conclusion

All the measurements have revealed that the Zn^{II}-assisted double helices of **5a**,**b** behaved not only as glue to connect two covalently linked nanorings but also as the fairly stable screws of hinges that exhibit thermally responsive synchronized spring motions. As observed in this investigation, dual-interlocked double helical assemblies assisted by metal cations are essential to form stimuli-responsive chiral macromolecular systems and materials.

Experimental Section

General procedures: The starting materials were purchased from Wako Chemical Co., Nacalai Chemical Co., and Aldrich Chemical Co. and used without further purification unless otherwise stated. UV/Vis spectra were recorded on a Hitachi U-3500 spectrometer. Fluorescence spectra and quantum yields were recorded on a Hitachi F-4500 fluorescence spectrometer for ordinary solutions and on a Hamamatsu Quantum Yields Measurements System for Organic LED Materials C9920-02, respectively. CD spectra were recorded on a JASCO J-720W spectrometer. NMR spectra used for the characterization of the products were recorded on a JEOL ECA-600 600 MHz spectrometer. All NMR spectra were referenced to solvent. Electrospray ionization mass spectra (ESIMS) were recorded on a Bruker microTOF spectrometer using positive- and negative-mode ESI-TOF methods. Matrix-assisted laser desorption/ionization time-of-flight mass spectra (MALDI-TOF MS) were recorded on a Shimadzu AXIMA-CFR plus spectrometer in the positive mode. Fast atom bombardment mass spectra (FABMS) were recorded using a JEOL GCmate instrument in the positive ion mode with a 3-nitrobenzylalcohol matrix. TLC analyses were carried out on aluminium sheets coated with silica gel 60 (Merck 5554). Column chromatography was performed on Sumitomo alumina KCG-1525, Wakogel C-200, and C-300.

5,5′-Diphenylbidipyrrin (Ph-BDPR): DDQ (49.2 mg, 0.22 mmol) was added to a toluene solution (15 mL) of a Ni^{II} complex of 5-phenyldipyrrin [(Ph-DPR)$_2$·Ni] (89.8 mg, 0.18 mmol) and the mixture was heated at reflux temperature for 12 h. The solvent was evaporated to dryness and the residue was purified by silica gel column chromatography (Wakogel C300, $CHCl_3$) and evaporated to afford the Ni^{II} complex of 5,5′-diphenylbidipyrrin [Ph-BDPR·Ni] as a brown solid. A 12 M aq. HCl (3 mL) solution was added to a $CHCl_3$ solution (5 mL) of [Ph-BDPR·Ni] (17.8 mg, 0.036 mmol) and the mixture was stirred at room temperature for 1 h. The reaction mixture was diluted with aq. $NaHCO_3$ (10 mL), dried over anhydrous Na_2SO_4, and evaporated to dryness. The solution was evaporated to afford Ph-BDPR (14.2 mg, 92 %) as a blue solid. R_f = 0.83 (CH_2Cl_2); ^{1}H NMR (600 MHz, $CDCl_3$, 20 °C): δ = 7.61 (t, J = 1.2 Hz, 2H; ArH), 7.55–7.54 (m, 4H; ArH), 7.51–7.46 (m, 6H; ArH), 7.00 (d, J = 4.2 Hz, 2H; pyrrole-H), 6.77 (d, J = 4.2 Hz, 2H; pyrrole-H), 6.58 (dd, J = 4.2, 1.2 Hz, 2H; pyrrole-H), 6.41 ppm (dd, J = 4.2, 1.8 Hz, 2H; pyrrole-H); UV/Vis ($CHCl_3$): λ_{max} ($\varepsilon \times 10^{-5}$) = 587 nm (0.23 M^{-1}cm^{-1}); MS (MALDI-TOF): m/z (%): calcd for $C_{30}H_{23}N_4$: 439.19 $[M+H]^+$; found: 439.1 (100), 440.1 (19).

Zn^{II} complex of Ph-BDPR (1a): [Zn(OAc)$_2$·2H$_2$O] (17.1 mg, 0.08 mmol) was added to a $CHCl_3$ solution (5 mL) of Ph-BDPR (14.2 mg, 0.032 mmol) and the mixture was stirred at room temperature for 3 h. The solvent was evaporated to dryness and the residue was purified by silica gel column chromatography (Wakogel C300, $CHCl_3$) and recrystallized from $CHCl_3$/hexane to afford **1a** (8.5 mg, 53 %) as a purple solid. R_f = 0.82 (CH_2Cl_2); ^{1}H NMR (600 MHz, $CDCl_3$, 20 °C): δ = 7.48–7.43 (m, 8H; ArH), 7.40–7.38 (m, 4H; ArH), 7.25–7.22 (m, 4H; ArH), 7.10 (d, J = 7.8 Hz, 4H; ArH), 7.06 (m, 4H; pyrrole-H), 6.57 (dd, J = 4.8, 1.2 Hz, 4H; pyrrole-H), 6.42 (d, J = 4.2 Hz, 4H; pyrrole-H), 6.37 (d, J = 4.2 Hz, 4H; pyrrole-H), 6.29 ppm (dd, J = 4.2, 1.2 Hz, 4H; pyrrole-H); UV/Vis ($CHCl_3$): λ_{max} ($\varepsilon \times 10^{-4}$) = 425 (5.5), 471 (1.8), 574 (3.5), 614 (3.2), 634 nm (3.1 M^{-1}cm^{-1}); MS (MALDI-TOF): m/z (%): calcd for $C_{80}H_{40}N_8Zn_2$: 1000.20 $[M]^+$; found: 1000.2 (46), 1001.2 (48), 1002.2 (96), 1003.2 (77), 1004.2 (100), 1005.3 (63), 1006.3 (42), 1007.2 (36), 1008.2 (19).

Zn^{II} complex of *p*Tol-BDPR (1b): [Zn(OAc)$_2$·2H$_2$O] (87.8 mg, 0.40 mmol) was added to a $CHCl_3$ solution (5 mL) of 5,5′-di(4-tolyl)bidipyrrin (*p*Tol-BDPR)[9b] (39.9 mg, 0.08 mmol) and the mixture was stirred at room temperature for 2 h. The solvent was evaporated to dryness and the residue was purified by silica gel column chromatography (Wakogel C300, $CHCl_3$) and recrystallized from $CHCl_3$/hexane to afford **1b** (41.1 mg, 90 %) as a purple solid. R_f = 0.84 (CH_2Cl_2); ^{1}H NMR (600 MHz, $CDCl_3$, 20 °C): δ = 7.35 (dd, J = 7.8, 1.8 Hz, 4H; ArH), 7.19 (d, J = 7.8 Hz, 4H; ArH), 7.04–7.03 (m, 4H; ArH), 7.00–6.98 (m, 8H; ArH, pyrrole-H), 6.58 (dd, J = 4.2, 1.2 Hz, 4H; pyrrole-H), 6.42 (d, J = 4.2 Hz, 4H; pyrrole-H), 6.36 (d, J = 3.6 Hz, 4H; pyrrole-H), 6.27 (dd, J = 4.2, 1.2 Hz, 4H; pyrrole-H), 2.45 ppm (s, 12H; CH_3); UV/Vis ($CHCl_3$): λ_{max} ($\varepsilon \times 10^{-5}$) = 425 (0.68), 470 (0.19), 574 (0.37), 614 (0.37), 634 nm (0.36 M^{-1}cm^{-1}); MS (MALDI-TOF): m/z (%): calcd for $C_{80}H_{40}N_8Zn_2$: 1056.26 $[M]^+$; found: 1056.3 (56), 1057.3 (45), 1058.3 (90), 1059.3 (73), 1060.3 (100), 1061.3 (70), 1062.3 (55), 1063.3 (36), 1064.3 (18), 1065.3 (10).

5-(3,4,5-Trihexadecyloxyphenyl)dipyrrin (3OC$_{16}$Ph-DPR): A THF solution (5 mL) of DDQ (26.5 mg, 0.116 mmol) was added to a THF solution (5 mL) of 5-(3,4,5-trihexadecyloxyphenyl)dipyrromethane[17] (100 mg, 0.106 mmol) and the mixture was stirred at room temperature for 30 min. The solvent was evaporated to dryness and the residue was purified by alumina (CH_2Cl_2) and silica gel column chromatography (Wakogel C300, CH_2Cl_2/hexane = 2:1) and recrystallized from $CHCl_3$/MeOH to afford 3OC$_{16}$Ph-DPR (61.3 mg, 0.096 mmol, 61 %) as an orange solid. R_f = 0.40 (CH_2Cl_2/hexane = 2:1); ^{1}H NMR (600 MHz, $CDCl_3$, 20 °C): δ = 7.63 (s, 2H; pyrrole-H), 6.71 (d, J = 4.2 Hz, 2H; pyrrole-H), 6.70 (s, 2H; ArH), 6.40 (m, 2H; pyrrole-H), 4.05–3.94 (m, 6H; OCH_2), 1.81–1.76 (m, 6H; CH_2), 1.51–1.25 (m, 78H; CH_2), 0.89–0.86 ppm (m, 9H; CH_3); UV/Vis (CH_2Cl_2): λ_{max} ($\varepsilon \times 10^{-5}$) = 437 nm (0.16 M^{-1}cm^{-1}); MS (MALDI-TOF): m/z (%): calcd for $C_{63}H_{108}N_2O_3$ $[M]^+$: 940.84; found: 940.8 (100), 941.8 (48).

Ni^{II} complex of 3OC$_{16}$Ph-DPR ([3OC$_{16}$Ph-DPR$_2$·Ni]): [Ni(OAc)$_2$·4H$_2$O] (707 mg, 2.84 mmol) was added to a $CHCl_3$ solution (20 mL) of 3OC$_{16}$Ph-DPR (1.337 g, 1.42 mmol) and the mixture was stirred at room temperature for 4 h. The mixture was then washed with brine, extracted with $CHCl_3$, and dried over anhydrous Na_2SO_4. The solvent was removed under vacuum and recrystallized from $CHCl_3$/MeOH to afford [3OC$_{16}$Ph-DPR$_2$·Ni] quantitatively as a metallic-green solid. R_f = 0.45 (CH_2Cl_2); ^{1}H NMR (600 MHz, $CDCl_3$, 20 °C): δ = 8.91 (s, 4H; pyrrole-H), 7.23 (d, J = 4.2 Hz, 4H; pyrrole-H), 6.84 (d, J = 4.2 Hz, 4H; pyrrole-H), 6.64 (s, 4H; phenyl-H), 4.05–3.92 (m, 12H; OCH_2), 1.81–1.76 (m, 12H; CH_2), 1.52–1.25 (m, 156H; CH_2), 0.89–0.86 ppm (m, 18H; CH_3); UV/Vis (CH_2Cl_2): λ_{max} ($\varepsilon \times 10^{-5}$) = 473 nm (0.43 M^{-1}cm^{-1}); MS (MALDI-TOF): m/z (%): calcd for $C_{126}H_{214}N_4NiO_6$ $[M]^+$: 1937.59; found: 1937.6 (80), 1938.6 (100), 1939.6 (84), 1940.6 (45), 1941.6 (22).

Ni^{II} complex of 5,5′-bis(3,4,5-trihexadecyloxyphenyl)bidipyrrin ([3OC$_{16}$Ph-BDPR·Ni]): *p*-Chloranil (12.5 mg, 0.051 mmol) was added to a toluene solution (30 mL) of [3OC$_{16}$Ph-DPR$_2$·Ni] (16.4 mg, 8.46 mmol) and the mixture was heated at reflux overnight. The solvent was evaporated to dryness and the residue was purified by silica gel column chromatography (Wakogel C300, CH_2Cl_2/hexane = 1:2) and recrystallized from CH_2Cl_2/MeOH to afford [3OC$_{16}$Ph-BDPR·Ni] (10.3 mg, 5.32 mmol, 63%) as a brown solid. R_f = 0.45 (CH_2Cl_2/hexane = 1:2); ^{1}H NMR (600 MHz, $CDCl_3$, 20°C): δ = 6.89 (m, 2H; pyrrole-H), 6.85 (d, J = 4.2 Hz, 2H; pyrrole-H), 6.77 (s, 4H; ArH), 6.62 (d, J = 4.2 Hz, 2H; pyrrole-H), 6.43 (m, 2H; pyrrole-H), 5.98 (s, 2H; pyrrole-H), 4.07–3.98 (m, 12H; OCH_2), 1.84–1.74 (m, 12H; CH_2), 1.53–1.25 (m, 156H; CH_2), 0.89–0.86 ppm (m, 18H; CH_3); UV/Vis (CH_2Cl_2): λ_{max} ($\varepsilon \times 10^{-5}$) = 419 nm (0.37 M^{-1}cm^{-1}); MS (MALDI-TOF): *m/z* (%): calcd for $C_{126}H_{212}N_4NiO_6$ $[M]^+$: 1935.57; found: 1935.6 (48), 1936.6 (100), 1937.6 (96), 1938.5 (87), 1939.6 (65), 1940.5 (40).

5,5′-Bis(3,4,5-trihexadecyloxyphenyl)bidipyrrin (3OC$_{16}$Ph-BDPR): A 12 M aq. HCl solution (20 mL) was added to a $CHCl_3$ solution (3 mL) of [3OC$_{16}$Ph-BDPR·Ni] (8.2 mg, 4.23 μmol) and the mixture was stirred at room temperature for 30 min. The mixture was then washed with Na_2CO_3, extracted with $CHCl_3$, and dried over anhydrous Na_2SO_4. The solvent was evaporated to dryness and the residue was recrystallized from $CHCl_3$/hexane to afford 3OC$_{16}$Ph-BDPR quantitatively as a green solid. R_f = 0.30 ($CHCl_3$); ^{1}H NMR (600 MHz, $CDCl_3$, 20°C): δ = 7.59 (s, 2H; pyrrole-H), 6.99 (d, J = 4.2 Hz, 2H; pyrrole-H), 6.88 (d, J = 4.2 Hz, 2H; pyrrole-H), 6.75 (s, 4H; ArH), 6.70 (m, 2H; pyrrole-H), 6.42 (m, 2H; pyrrole-H), 4.07–3.97 (m, 12H; OCH_2), 1.83–1.78 (m, 12H; CH_2), 1.53–1.25 (m, 158H; CH_2), 0.89–0.86 ppm (m, 18H; CH_3); UV/Vis ($CHCl_3$): λ_{max} ($\varepsilon \times 10^{-5}$) = 594 nm (0.46 M^{-1}cm^{-1}); MS (MALDI-TOF): *m/z* (%): calcd for $C_{126}H_{214}N_4O_6$ $[M+H]^+$: 1880.66; found: 1879.7 (67), 1880.7 (100).

Zn^{II} complex of 3OC$_{16}$Ph-BDPR ([3OC$_{16}$Ph-BDPR$_2$·Zn$_2$], 1c): [Zn(OAc)$_2$·2H$_2$O] (94 mg, 0.432 mmol) was added to a $CHCl_3$ (15 mL) solution of 3OC$_{16}$Ph-BDPR (203.7 mg, 0.108 mmol) and the mixture was stirred at room temperature for 3 h. The mixture was then washed with brine, extracted with $CHCl_3$, dried over anhydrous Na_2SO_4, and evaporated to dryness. The residue was recrystallized from $CHCl_3$/hexane to afford [3OC$_{16}$Ph-BDPR$_2$·Zn$_2$] (184.6 mg, 0.095 mmol, 88%) as a green solid. R_f = 0.30 (CH_2Cl_2/hexane = 1:2); ^{1}H NMR (600 MHz, $CDCl_3$, 20°C): δ = 6.86 (s, 4H; pyrrole-H), 6.72 (d, J = 1.2 Hz, 4H; ArH), 6.70 (d, J = 4.2 Hz, 4H; pyrrole-H), 6.47 (d, J = 4.2 Hz, 4H; pyrrole-H), 6.42 (d, J = 4.2 Hz, 4H; pyrrole-H), 6.32 (d, J = 1.2 Hz, 4H; ArH), 6.21 (m, 4H; pyrrole-H), 3.99–3.91 (m, 16H; OCH_2), 3.52–3.50 (m, 4H; OCH_2), 2.94–2.90 (m, 4H; OCH_2), 1.80–1.76 (m, 16H; CH_2), 1.64–1.24 (m, 292H; CH_2), 0.89–0.86 ppm (m, 36H; CH_3); UV/Vis ($CHCl_3$): λ_{max} ($\varepsilon \times 10^{-5}$) = 427 nm (1.35 M^{-1}cm^{-1}); MS (MALDI-TOF): *m/z* (%): calcd for $C_{252}H_{424}N_8O_{12}Zn_2$: 3883.14 $[M]^+$; found: 3883.1 (18), 3884.1 (36), 3885.0 (66), 3886.0 (76), 3887.0 (92), 3888.0 (100), 3888.9 (82), 3889.9 (55), 3890.9 (42), 3891.9 (16).

5-(3,4,5-Tri-TEG-phenyl)dipyrromethane (3TEGPh-DPM): 3,4,5-Tri-TEG-benzaldehyde[18] (1.78 g, 2.93 mmol) was dissolved in pyrrole (1.22 mL, 17.6 mmol) and CH_2Cl_2 (10 mL) and degassed by bubbling with nitrogen for 30 min. Trifluoroacetic acid (22 mL, 0.293 mmol) was added and the solution was stirred under N_2 at room temperature for 30 min and then quenched with triethylamine (1 mL). The remaining pyrrole was removed by vacuum distillation with gentle heating. The residue was purified by silica gel column chromatography (Wakogel C300, 5% MeOH/CH_2Cl_2) to afford 3TEGPh-DPM (284.4 mg, 0.40 mmol, 14%) as a yellow oil. R_f = 0.50 (5% MeOH/CH_2Cl_2); ^{1}H NMR (600 MHz, $CDCl_3$, 20°C): δ = 8.10 (s, 2H; NH), 6.69 (m, 2H; pyrrole-H), 6.48 (s, 2H; ArH), 6.14 (m, 2H; pyrrole-H), 5.92 (s, 2H; pyrrole-H), 5.36 (s, 1H; *meso*-H), 4.12–4.07 (m, 6H; OCH_2), 3.79–3.52 (m, 30H; CH_2), 3.37–3.36 ppm (m, 9H; CH_3); MS (MALDI-TOF): *m/z* (%): calcd for $C_{36}H_{56}N_2O_{12}$: 708.38 $[M]^+$; found: 708.4 (100), 709.4 (38).

5-(3,4,5-Tri-TEG-phenyl)dipyrrin (3TEGPh-DPR): A THF solution (15 mL) of DDQ (100 mg, 0.44 mmol) was added to a THF solution (15 mL) of 3TEGPh-DPM (284.4 mg, 0.40 mmol) and the mixture was stirred at room temperature for 15 min. The solvent was evaporated to dryness and the residue was purified by alumina (CH_2Cl_2) and silica gel column chromatography (Wakogel C300, 7% MeOH/CH_2Cl_2) to afford 3TEGPh-DPR (202.6 mg, 0.29 mmol, 72%) as an orange oil. R_f = 0.25 (7% MeOH/CH_2Cl_2); ^{1}H NMR (600 MHz, $CDCl_3$, 20°C): δ = 7.63 (s, 2H; ArH), 6.75 (s, 2H; pyrrole-H), 6.67 (d, J = 4.2 Hz, 2H; pyrrole-H), 6.40 (d, J = 4.2 Hz, 2H; pyrrole-H), 4.26–4.14 (m, 6H; OCH_2), 3.86–3.52 (m, 30H; CH_2), 3.38–3.36 ppm (m, 9H; CH_3); UV/Vis ($CHCl_3$): λ_{max} ($\varepsilon \times 10^{-5}$) = 437 nm (0.09 M^{-1}cm^{-1}); MS (MALDI-TOF): *m/z* (%): calcd for $C_{36}H_{54}N_2O_{12}$: 706.37 $[M]^+$; found: 706.4 (100), 707.4 (35).

Ni^{II} complex of 3TEGPh-DPR ([3TEGPh-DPR$_2$·Ni]): [Ni(OAc)$_2$·4H$_2$O] (286 mg, 1.15 mmol) and Na_2CO_3 (158 mg, 1.15 mmol) were added to a $CHCl_3$ solution (15 mL) of 3TEGPh-DPR (202.6 mg, 0.29 mmol) and the mixture was stirred at room temperature overnight. The mixture was then washed with brine, extracted with CH_2Cl_2, and dried over anhydrous Na_2SO_4. The solvent was removed under vacuum to afford 3TEGPh-DPR (168.6 mg, 0.11 mmol, 80%) as an orange solid. R_f = 0.25 (7% MeOH/CH_2Cl_2); ^{1}H NMR (600 MHz, $CDCl_3$, 20°C): δ = 8.84 (s, 4H; pyrrole-H), 7.20 (s, 4H; pyrrole-H), 6.81 (d, J = 3.0 Hz, 4H; pyrrole-H), 6.69 (s, 4H; ArH), 4.24–4.13 (m, 12H; OCH_2), 3.84–3.54 (m, 60H; CH_2), 3.38–3.37 ppm (m, 18H; CH_3); UV/Vis ($CHCl_3$): λ_{max} ($\varepsilon \times 10^{-5}$) = 475 nm (0.31 M^{-1}cm^{-1}); MS (MALDI-TOF): *m/z* (%): calcd for $C_{72}H_{106}N_4NiO_{24}$: 1468.65 $[M]^+$; found: 1468.7 (100), 1469.7 (98), 1470.7 (76), 1471.6 (48), 1472.7 (22).

Ni^{II} complex of 5,5′-bis(3,4,5-tri-TEG-phenyl)bidipyrrin ([3TEGPh-BDPR·Ni]): *p*-Chloranil (158 mg, 0.645 mmol) was added to a toluene solution (150 mL) of [3TEGPh-DPR$_2$·Ni] (158 mg, 0.107 mmol) and the mixture was heated at reflux overnight. The solvent was then evaporated to dryness and the residue was purified by silica gel column chromatography (Wakogel C300, 3% MeOH/CH_2Cl_2) to afford [3TEGPh-BDPR·Ni] (76.9 mg, 0.052 mmol, 49%) as a brown solid. R_f = 0.60 (3% MeOH/CH_2Cl_2); ^{1}H NMR (600 MHz, $CDCl_3$, 20°C): δ = 6.85 (m, 2H; pyrrole-H), 6.82 (s, 4H; ArH), 6.81 (s, 2H; pyrrole-H), 6.63 (d, J = 4.2 Hz, 2H; pyrrole-H), 6.43 (m, 2H; pyrrole-H), 5.96 (s, 2H; pyrrole-H), 4.27–4.18 (m, 12H; OCH_2), 3.88–3.53 (m, 60H; CH_2), 3.39–3.36 ppm (m, 18H; CH_3); UV/Vis (CH_2Cl_2): λ_{max} ($\varepsilon \times 10^{-5}$) = 416 nm (0.29 M^{-1}cm^{-1}); MS (MALDI-TOF): *m/z* (%): calcd for $C_{72}H_{104}N_4NiO_{24}$: 1466.64 $[M]^+$; found: 1466.6 (100), 1467.6 (88), 1468.7 (54), 1469.7 (26).

5,5′-Bis(3,4,5-tri-TEG-phenyl)bidipyrrin (3TEGPh-BDPR): TFA (3 mL) was added to a $CHCl_3$ solution (30 mL) of [3TEGPh-BDPR·Ni] (70 mg, 0.048 mmol) and the mixture was stirred at room temperature for 3 h. The mixture was then washed with Na_2CO_3, extracted with $CHCl_3$, and dried over anhydrous Na_2SO_4. The solvent was evaporated to dryness and the residue was purified by silica gel column chromatography (Wakogel C300, 4% MeOH/CH_2Cl_2) to afford 3TEGPh-BDPR (30.9 mg, 0.022 mmol, 46%) as a green solid. R_f = 0.40 (6% MeOH/CH_2Cl_2); ^{1}H NMR (600 MHz, $CDCl_3$, 20°C): δ = 7.60 (s, 2H; pyrrole-H), 6.99 (d, J = 4.2 Hz, 2H; pyrrole-H), 6.84 (d, J = 4.2 Hz, 2H; pyrrole-H), 6.80 (s, 4H; ArH), 6.65 (m, 2H; pyrrole-H), 6.41 (m, 2H; pyrrole-H), 4.26–4.17 (m, 12H; OCH_2), 3.87–3.52 (m, 60H; CH_2), 3.39–3.36 ppm (m, 18H; CH_3); UV/Vis ($CHCl_3$): λ_{max} ($\varepsilon \times 10^{-5}$) = 593 nm (0.40 M^{-1}cm^{-1}); MS (MALDI-TOF): *m/z* (%): calcd for $C_{72}H_{106}N_4O_{24}$: 1410.72 $[M]^+$; found: 1410.7 (100), 1411.7 (70).

Zn^{II} complex of 3TEGPh-DPR ([3TEGPh-DPR$_2$·Zn$_2$], 1d): [Zn(OAc)$_2$·2H$_2$O] (16.8 mg, 0.0764 mmol) was added to a CH_2Cl_2 solution (20 mL) of 3TEGPh-BDPR (27 mg, 0.0191 mmol) and the mixture was stirred at room temperature for 3 h. The mixture was then washed with brine, extracted with CH_2Cl_2, dried over anhydrous Na_2SO_4, and evaporated to dryness. The residue was purified by silica gel column chromatography (Wakogel C300, 15% MeOH/CH_2Cl_2) to afford [3TEGPh-DPR$_2$·Zn$_2$] (15.6 mg, 5.27 μmol, 55%) as a green solid. R_f = 0.75 (15% MeOH/CH_2Cl_2); ^{1}H NMR (600 MHz, $CDCl_3$, 20°C): δ = 6.83 (s, 4H; pyrrole-H), 6.75 (d, J = 1.2 Hz, 4H; pyrrole-H), 6.62 (d, J = 4.2 Hz, 4H; pyrrole-H), 6.44 (s, 8H; ArH), 6.30 (d, J = 1.8 Hz, 4H; pyrrole-H), 6.21 (m, 4H; pyrrole-H), 4.21–4.10 (m, 16H; OCH_2), 3.83–3.50 (m, 124H; CH_2), 3.39–3.34 (m, 36H; CH_3), 3.25–3.24 ppm (m, 4H; CH_2); UV/Vis ($CHCl_3$): λ_{max} ($\varepsilon \times 10^{-5}$) = 427 nm (0.72 M^{-1}cm^{-1}); MS (MALDI-TOF): *m/z* (%): calcd for $C_{144}H_{208}N_8O_8Zn_2$ $[M]^+$: 2945.26; found: 2945.3 (14), 2946.3 (38),

2947.3 (61), 2948.3 (78), 2949.3 (100), 2950.3 (88), 2951.3 (68), 2952.3 (53), 2953.3 (32), 2954.3 (16), 2955.3 (8).

2-*tert*-Butyl-1,3-bis(3-formylphenylethynyl)benzene (*t*BuPh-*mmm*-FOR): A mixture of 3-bromobenzaldehyde (0.38 g, 2.04 mmol), 1-*tert*-butyl-3,5-diethynylbenzene (0.35 g, 1.92 mmol), triethylamine (0.3 mL, 4.1 mmol), $[PdCl_2(PPh_3)_2]$ (17.5 mg, 0.02 mmol), triphenylphosphine (3.8 mg, 0.01 mmol), and CuI (1 mg, 0.005 mmol) in dry THF (10 mL) was heated at reflux under nitrogen for 64 h. The reaction mixture was diluted with CH_2Cl_2 (50 mL), washed with 0.01 M aq. EDTA (80 mL), dried over Na_2SO_4, and evaporated to dryness. The residue was purified by silica gel column chromatography (Wakogel C300, 30% hexane/CH_2Cl_2) and recrystallized from CH_2Cl_2/hexane to afford *t*BuPh-*mmm*-FOR (72.1 mg, 24%) as a dark-red oil. R_f=0.47 (CH_2Cl_2); ^{1}H NMR (600 MHz, $CDCl_3$, 20°C): δ=10.03 (s, 2H; CHO), 8.06 (s, 2H; ArH), 7.87 (d, J=7.8 Hz, 2H; ArH), 7.79 (d, J=7.8 Hz, 2H; ArH), 7.57–7.54 (m, 5H; ArH), 1.37 ppm (s, 9H; CH_3); MS (FAB): m/z (%): calcd for $C_{28}H_{22}O_2$: 390.16 $[M]^+$; found: 389.7 (100), 390.7 (97).

2-*tert*-Butyl-1,3-bis(3-dipyrrolylmethylphenylethynyl)benzene (*t*BuPh-*mmm*-DPM): Aldehyde *t*BuPh-*mmm*-FOR (120 mg, 0.31 mmol) was dissolved in pyrrole (6.0 mL) and degassed by bubbling with nitrogen for 10 min. Trifluoroacetic acid (6.0 μL, 0.035 mmol) was added and the solution was stirred under N_2 at room temperature for 40 min and then quenched with triethylamine (0.4 mL). The remaining pyrrole was removed by vacuum distillation with gentle heating. The residue was purified by silica gel column chromatography (Wakogel C300, 1% Et_3N/CH_2Cl_2) and recrystallized from CH_2Cl_2/hexane to afford *t*BuPh-*mmm*-DPM (117 mg, 61%) as a light-yellow solid. R_f=0.44 (CH_2Cl_2); ^{1}H NMR (600 MHz, $CDCl_3$, 20°C): δ=7.98 (brs, 4H; NH), 7.49–7.21 (m, 11H; ArH), 6.73 (m, 4H; pyrrole-H), 6.17 (m, 4H; pyrrole-H), 5.94 (m, 4H; pyrrole-H), 5.49 (s, 2H; *meso*-H), 1.33 ppm (s, 9H; CH_3); MS (FAB): m/z (%): calcd for $C_{44}H_{38}N_4$: 622.31 $[M]^+$; found: 622.4 (100), 623.4 (71).

2-*tert*-Butyl-1,3-bis(dipyrrolylphenylethynyl)benzene (*t*BuPh-*mmm*-DPR): DDQ (28.0 mg, 0.12 mmol) was added to a THF solution (15 mL) of dipyrromethane *t*BuPh-*mmm*-DPM (38.4 mg, 0.06 mmol) and the mixture was stirred at 0°C for 20 min. The solvent was evaporated to dryness and the residue was purified by alumina (5% MeOH/CH_2Cl_2) and silica gel column chromatography (Wakogel C200; 5% MeOH/CH_2Cl_2) to afford *t*BuPh-*mmm*-DPR (37.3 mg, 98%) as a brown solid. R_f=0.24 (CH_2Cl_2); ^{1}H NMR (600 MHz, $CDCl_3$, 20°C): δ=7.69–7.44 (m, 15H; ArH, pyrrole-H), 6.61 (m, 4H; pyrrole-H), 6.41 (m, 4H; pyrrole-H), 1.34 ppm (s, 9H; CH_3); UV/Vis ($CHCl_3$): λ_{max} ($\varepsilon\times10^{-5}$)=435 nm (0.30 $M^{-1}cm^{-1}$); MS (FAB): m/z (%): calcd for $C_{44}H_{34}N_4$: 618.28 $[M]^+$; found: 619.0 (100), 620.0 (65).

Ni^{II} complex of *t*BuPh-*mmm*-DPR (2b): Pyrene (3.9 mg, 0.02 mmol) and $[Ni(OAc)_2{\cdot}4H_2O]$ (9.6 mg, 0.04 mmol) were added to a $CHCl_3$ solution (20 mL) of dipyrrin *t*BuPh-*mmm*-DPR (23.9 mg, 0.04 mmol) and the mixture was heated at reflux for 46 h. The solvent was evaporated to dryness and the residue was purified by silica gel column chromatography (Wakogel C200; 3% MeOH/$CHCl_3$) and recrystallized from $CHCl_3$/hexane to afford **2b** (17.1 mg, 66%) as a white solid. R_f=0.90 (5% MeOH/CH_2Cl_2); ^{1}H NMR (600 MHz, $CDCl_3$, 20°C): δ=9.34 (brs, 8H; pyrrole-H), 7.62–7.57 (m, 10H; ArH, pyrrole-H), 7.52 (m, 4H; ArH), 7.44–7.43 (m, 4H; ArH), 7.41–7.36 (m, 8H; ArH), 6.77 (brs, 8H; pyrrole-H), 1.37 ppm (s, 18H; CH_3); UV/Vis ($CHCl_3$): λ_{max} ($\varepsilon\times10^{-5}$)=478 nm (0.92 $M^{-1}cm^{-1}$); MS (MALDI-TOF): m/z (%, observed with the use of 2,5-dihydroxybenzoic acid as matrix): calcd for $C_{88}H_{64}N_8Ni_2$: 1348.40 $[M]^+$; found: 1348.1 (14), 1349.4 (60), 1350.4 (81), 1351.5 (95), 1352.5 (100), 1353.5 (67), 1354.5 (51), 1355.5 (28).

Ni^{II} complex of cyclic bis-bidipyrrin cBDPR (3a): *p*-Chloranil (403.0 mg, 1.64 mmol) was added to a $CHCl_3$ solution (40 mL) of **2a**[12b] (202.7 mg, 0.16 mmol) and the mixture was heated at reflux for 46 h. The solution was purified by alumina ($CHCl_3$) and silica gel column chromatography (Wakogel C300, $CHCl_3$) and recrystallized from $CHCl_3$/hexane to afford **3a** (171.8 mg, 85%) as a brown solid. R_f=0.85 (CH_2Cl_2); ^{1}H NMR (600 MHz, $CDCl_3$, 20°C): δ=7.75 (s, 2H; ArH), 7.72 (s, 4H; ArH), 7.65 (dt, J=7.2, 1.2 Hz, 4H; ArH), 7.54–7.52 (m, 8H; ArH), 7.46 (dd, J=7.8, 7.2 Hz, 4H; ArH), 7.38 (t, J=7.8 Hz, 2H; ArH), 6.83 (dd, J=4.8, 1.2 Hz, 4H; pyrrole-H), 6.68 (m, 4H; pyrrole-H), 6.62 (d, J=2.4 Hz, 4H; pyrrole-H), 6.44 (dd, J=4.2, 2.4 Hz, 4H; pyrrole-H), 5.96 ppm (brs, 4H; pyrrole-H); UV/Vis ($CHCl_3$): λ_{max} ($\varepsilon\times10^{-5}$)=412 (0.68), 575 (0.22), 845 nm (0.17 $M^{-1}cm^{-1}$); MS (MALDI-TOF): m/z (%): calcd for $C_{80}H_{44}N_8Ni_2$: 1232.24 $[M]^+$; found: 1232.2 (56), 1233.2 (69), 1234.2 (100), 1235.2 (81), 1236.2 (64), 1237.2 (45), 1238.2 (15), 1239.2 (13), 1240.2 (7).

Ni^{II} complex of the mono-oxidative coupling derivative of bis-bidipyrrin ([4′a·Ni$_2$]): The fraction following that of **3a** was recrystallized from $CHCl_3$/hexane to afford [**4′a**·Ni_2] (21.5 mg, 10%) as a brown solid. R_f=0.32 (CH_2Cl_2); ^{1}H NMR (600 MHz, $CDCl_3$, 20°C): δ=9.12 (s, 4H; pyrrole-H), 7.77–7.72 (m, 4H; ArH), 7.68–7.60 (m, 10H; ArH, pyrrole-H), 7.55–7.43 (m, 8H; ArH), 7.40–7.34 (m, 6H; ArH), 6.83–6.70 (m, 6H; pyrrole-H), 6.65 (d, J=4.2 Hz, 2H; pyrrole-H), 6.61 (d, J=4.2 Hz, 2H; pyrrole-H), 6.46 (dd, J=4.2, 1.2 Hz, 2H; pyrrole-H), 6.41 (dd, J=3.6, 1.2 Hz, 2H; pyrrole-H), 5.98 ppm (m, 2H; pyrrole-H); UV/Vis ($CHCl_3$): λ_{max} ($\varepsilon\times10^{-5}$)=430 (0.61), 560 (0.14), 845 nm (0.11 $M^{-1}cm^{-1}$); MS (MALDI-TOF): m/z (%): calcd for $C_{80}H_{46}N_8Ni_2$: 1234.26 $[M]^+$; found: 1234.3 (53), 1234.3 (66), 1235.3 (100), 1236.3 (72), 1237.3 (43).

Ni^{II} complex of *t*BuPh-cBDPR (3b): *p*-Chloranil (173.6 mg, 7.10 mmol) was added to a $CHCl_3$ solution (14 mL) of **2b** (95.4 mg, 0.07 mmol) and the mixture was heated at reflux for 50 h. The solvent was evaporated to dryness and the residue was purified by alumina ($CHCl_3$) and silica gel column chromatography (Wakogel C300, $CHCl_3$) and recrystallized from $CHCl_3$/hexane to afford **3b** (87.3 mg, 92%) as a brown solid. R_f=0.86 (CH_2Cl_2); ^{1}H NMR (600 MHz, $CDCl_3$, 20°C): δ=7.72 (s, 4H; ArH), 7.66 (dt, J=7.8, 1.2 Hz, 4H; ArH), 7.57–7.51 (m, 12H; ArH), 7.46 (dd, J=7.8, 7.2 Hz, 4H; ArH), 6.84 (dd, J=4.2, 1.2 Hz, 4H; pyrrole-H), 6.68 (m, 4H; pyrrole-H), 6.61 (m, 4H; pyrrole-H), 6.44 (dd, J=4.2, 1.2 Hz, 4H; pyrrole-H), 5.96 (m, 4H; pyrrole-H), 1.38 ppm (s, 18H; CH_3); UV/Vis ($CHCl_3$): λ_{max} ($\varepsilon\times10^{-5}$)=414 (0.79), 565 (0.27), 846 nm (0.21 $M^{-1}cm^{-1}$); MS (MALDI-TOF): m/z (%): calcd for $C_{88}H_{60}N_8Ni_2$: 1344.36: $[M]^+$; found: 1344.4 (53), 1345.4 (76), 1346.4 (100), 1347.4 (78), 1348.4 (57), 1349.4 (33), 1350.4 (14).

Cyclic bis-bidipyrrin cBDPR (4a): A 12 M aq. HCl solution (10 mL) was added to a $CHCl_3$ solution (10 mL) of **3a** (69.7 mg, 0.056 mmol) and the mixture was stirred at room temperature for 1 h. The reaction mixture was then diluted with aq. $NaHCO_3$ (50 mL), dried over Na_2SO_4, and evaporated to dryness. The solution was recrystallized from $CHCl_3$/hexane to afford **4a** (58.4 mg, 92%) as a blue solid. R_f=0.11 (CH_2Cl_2); ^{1}H NMR (600 MHz, $CDCl_3$, 20°C): δ=7.72–7.65 (m, 14H; ArH), 7.54–7.42 (m, 12H; ArH), 7.38 (t, J=7.8 Hz, 4H; ArH), 6.87 (brs, 2H; pyrrole-H), 6.78 (brs, 2H; pyrrole-H), 6.65 (brs, 2H; pyrrole-H), 6.60 (brs, 2H; pyrrole-H), 6.45 (brs, 2H; pyrrole-H), 6.32 ppm (brs, 2H; pyrrole-H); UV/Vis ($CHCl_3$): λ_{max} ($\varepsilon\times10^{-5}$)=410 (0.49), 587 (0.66), 724 nm (0.34 $M^{-1}cm^{-1}$); MS (ESI-TOF): m/z (%): calcd for $C_{80}H_{49}N_8$: 1121.41 $[M+H]^+$; found: 1121.41 (100), 1122.42 (92), 1123.42 (38), 1124.43 (15).

Cyclic bis-bidipyrrin *t*BuPh-cBDPR (4b): A 12 M aq. HCl solution (5 mL) was added to a $CHCl_3$ solution (5 mL) of **3b** (35.5 mg, 0.026 mmol) and the mixture was stirred at room temperature for 1 h. The reaction mixture was then diluted with aq. $NaHCO_3$ (20 mL), dried over Na_2SO_4, and evaporated to dryness. The solution was recrystallized from $CHCl_3$/hexane to afford **4b** (26.8 mg, 83%) as a blue solid. R_f=0.12 (CH_2Cl_2); ^{1}H NMR (600 MHz, $CDCl_3$, 20°C): δ=7.72–7.65 (m, 8H; ArH), 7.57–7.55 (m, 6H; ArH), 7.50–7.49 (m, 4H; ArH), 7.46 (t, J=7.8 Hz, 4H; ArH), 6.87 (brs, 2H; pyrrole-H), 6.78 (brs, 2H; pyrrole-H), 6.66 (brs, 2H; pyrrole-H), 6.60 (brs, 2H; pyrrole-H), 6.45 (brs, 2H; pyrrole-H), 6.32 (brs, 2H; pyrrole-H), 1.39 ppm (s, 18H; CH_3); UV/Vis ($CHCl_3$): λ_{max} ($\varepsilon\times10^{-5}$)=411 (0.52), 588 nm (0.66 $M^{-1}cm^{-1}$); MS (MALDI-TOF): m/z (%): calcd for $C_{88}H_{65}N_8$: 1233.53 $[M+H]^+$: 1233.5 (100), 1234.5 (82), 1235.5 (44), 1236.5 (12).

Cu^{II} complex of cBDPR (3′a): $Cu(OAc)_2$ (24.6 mg, 0.14 mmol) was added to a $CHCl_3$ solution (5 mL) of bidipyrrin **4a** (15.2 mg, 0.014 mmol) and the mixture was stirred for 25 h at room temperature. The solvent was evaporated to dryness and the residue was purified by silica gel column chromatography (Wakogel C300, $CHCl_3$) and recrystallized from $CHCl_3$/hexane to afford **3′a** (8.4 mg, 50%) as an orange solid. R_f=0.81 (CH_2Cl_2); UV/Vis ($CHCl_3$): λ_{max} ($\varepsilon\times10^{-5}$)=467 (0.69), 769 nm (0.49 $M^{-1}cm^{-1}$); MS (MALDI-TOF): m/z (%): calcd for $C_{80}H_{44}N_8Cu_2$:

1242.23 $[M]^+$; found: 1242.2 (83), 1243.2 (78), 1244.2 (100), 1245.2 (80), 1246.2 (44), 1247.2 (24), 1248.2 (8).

Zn^{II} complex of cBDPR (5a): $[Zn(OAc)_2{\cdot}2H_2O]$ (7.6 mg, 0.03 mmol) was added to a $CHCl_3$ solution (13 mL) of bidipyrrin **4a** (21.1 mg, 0.03 mmol) and the mixture was stirred for 25 h at room temperature. The solvent was evaporated to dryness and the residue was purified by silica gel column chromatography (Wakogel C300, $CHCl_3$) and recrystallized from $CHCl_3$/hexane to afford **5a** (15.8 mg, 68%) as a green solid. $R_f=0.82$ (CH_2Cl_2); ^{1}H NMR (600 MHz, $CDCl_3$, 20°C): $\delta=7.68$ (s, 4H; ArH), 7.53–7.50 (m, 8H; ArH), 7.44 (d, $J=7.8$ Hz, 4H; ArH), 7.39 (dd, $J=7.8$, 7.2 Hz, 4H; ArH), 7.33–7.29 (m, 8H; ArH), 7.22 (dt, $J=8.4$, 1.2 Hz, 4H; ArH), 7.17 (s, 4H; ArH), 7.13 (d, $J=4.2$ Hz, 4H; pyrrole-H), 7.04 (s, 4H; pyrrole-H), 6.99 (dd, $J=7.8$, 7.2 Hz, 4H; ArH), 6.93 (d, $J=7.8$ Hz, 4H; ArH), 6.75 (s, 4H; pyrrole-H), 6.67 (d, $J=3.6$ Hz, 4H; pyrrole-H), 6.40–6.38 (m, 12H; pyrrole-H), 6.34 (d, $J=4.2$ Hz, 4H; pyrrole-H), 6.30 (d, $J=4.2$ Hz, 4H; pyrrole-H), 6.28 ppm (d, $J=4.2$ Hz, 4H; pyrrole-H); UV/Vis ($CHCl_3$): λ_{max} ($\varepsilon\times10^{-5}$)=424 (2.13), 655 nm ($0.84\,M^{-1}cm^{-1}$); MS (MALDI-TOF): m/z (%): calcd for $C_{160}H_{88}N_{16}Zn_4$: 2488.45 $[M]^+$; found: 2488.4 (6), 2489.3 (14), 2490.4 (31), 2491.4 (46), 2492.4 (70), 2493.3 (79), 2494.3 (98), 2495.3 (100), 2496.3 (100), 2497.3 (80), 2498.3 (72), 2499.3 (52), 2500.3 (38), 2501.3 (27), 2502.4 (14), 2503.3 (8).

Zn^{II} complex of *t*BuPh-cBDPR (5b): $[Zn(OAc)_2{\cdot}2H_2O]$ (38.8 mg, 0.18 mmol) was added to a $CHCl_3$ solution (7 mL) of bidipyrrin **4b** (21.8 mg, 0.018 mmol) and the mixture was stirred for 13 h at room temperature. The solvent was evaporated to dryness and the residue was purified by silica gel column chromatography (Wakogel C300, $CHCl_3$) and recrystallized from $CHCl_3$/hexane to afford **5b** (15.8 mg, 68%) as a green solid. $R_f=0.64$ (CH_2Cl_2); ^{1}H NMR (600 MHz, $CDCl_3$, 20°C): $\delta=7.69$ (s, 4H; ArH), 7.54–7.51 (m, 8H; ArH), 7.46 (t, $J=1.8$ Hz, 4H; ArH), 7.39 (t, $J=7.8$ Hz, 4H; ArH), 7.34 (dt, $J=8.4$, 1.2 Hz, 8H; ArH), 7.17 (dt, $J=9.0$, 1.2 Hz, 8H; ArH), 7.13 (dd, $J=4.2$, 0.6 Hz, 4H; pyrrole-H), 7.05 (t, $J=1.2$ Hz, 4H; pyrrole-H), 6.98 (t, $J=7.2$ Hz, 4H; ArH), 6.92 (dt, $J=7.2$, 1.8 Hz, 4H; ArH), 6.73 (m, 4H; pyrrole-H), 6.69 (dd, $J=4.2$, 1.2 Hz, 4H; pyrrole-H), 6.39–6.37 (m, 12H; pyrrole-H), 6.31–6.28 (m, 12H; pyrrole-H), 1.37 ppm (s, 36H; CH_3); UV/Vis ($CHCl_3$): λ_{max} ($\varepsilon\times10^{-5}$)=425 (1.83), 651 nm ($0.81\,M^{-1}cm^{-1}$); MS (MALDI-TOF): m/z (%): calcd for $C_{176}H_{120}N_{16}Zn_4$: 2712.70 $[M]^+$; found: 2712.7 (3), 2713.8 (5), 2714.8 (10), 2715.8 (24), 2716.8 (37), 2717.8 (60), 2718.8 (74), 2719.8 (94), 2720.7 (100), 2721.8 (98), 2722.7 (92), 2723.7 (78), 2724.7 (56), 2725.7 (40), 2726.7 (27), 2727.7 (15), 2728.7 (11), 2729.7 (6), 2730.7 (4).

Structure optimization: DFT calculations on **1a** and **5a** were carried out by using the Gaussian 03 software package[14] and an HP Compaq dc5100 SFF computer.

X-ray crystallography: Data was collected on a Rigaku RAXIS-RAPID diffractometer for **1a**, refined by full-matrix least-squares procedures with anisotropic thermal parameters for the non-hydrogen atoms. The hydrogen atoms were calculated in ideal positions. Structures were solved by using the Crystal Structure crystallographic software package[19] and SIR97,[20] and refined by full-matrix least-squares on F^2 with anisotropic displacement parameters for the non-hydrogen atoms using SHELXL-97.[21] Crystals of **1a** were obtained from CH_2Cl_2. Crystal data for **1a** (123 K): $C_{60}H_{40}N_8Zn_2$, $M_w=1003.74$, monoclinic, $P2_1/n$ (no. 14), $a=13.345(3)$, $b=16.390(3)$, $c=22.258(5)$ Å, $\beta=101.737(9)°$, $V=4766.8(19)$ Å^3, $T=123(2)$ K, $Z=4$, $\rho_{calcd}=1.399\,g\,cm^{-3}$, $\mu(Mo_{K\alpha})=1.057\,mm^{-1}$, reflections collected=44617, independent reflections=10893, $R_1=0.0355$, $wR_2=0.0799$, GOF=1.023 [$I>2\sigma(I)$]. Crystal data for **1a** (293 K): $C_{60}H_{40}N_8Zn_2$, $M_w=1003.74$, monoclinic, $P2_1/n$ (no. 14), $a=13.453(3)$, $b=16.452(3)$, $c=22.320(6)$ Å, $\beta=101.137(9)°$, $V=4846.9(19)$ Å^3, $T=293(2)$ K, $Z=4$, $\rho_{calcd}=1.376\,g\,cm^{-3}$, $\mu(Mo_{K\alpha})=1.039\,mm^{-1}$, reflections collected=46924, independent reflections=11081, $R_1=0.0407$, $wR_2=0.0899$, GOF=1.016 [$I>2\sigma(I)$].

CCDC-768146 and -768147 contain the supplementary crystallographic data for this paper. These data can be obtained free of charge from The Cambridge Crystallographic Data Centre via www.ccdc.cam.ac.uk/data_request/cif.

X-ray powder diffraction experiments: High-resolution XRD analysis was carried out by using a synchrotron radiation X-ray beam with a wavelength of 1.00 Å on BL40B2 at SPring-8 (Hyogo, Japan). A large Debye–Scherrer camera with a camera length of 543 mm was used with an imaging plate as detector and the diffraction pattern was obtained with a 0.01° step in 2θ. The exposure time of the X-ray beam was 10 s for the melted sample of **1c** sealed in a quartz capillary.

Dynamic light scattering: DLS measurements were taken with a Malvern Zetasizer Nano-ZS differential light-scattering instrument.

HPLC: Chiral HPLC analyses were performed with a Shimadzu LC-20A instrument with Daicel Chiralpak IA column.

Time-resolved fluorescence decay measurements: Time-resolved fluorescence lifetime experiments were performed by the time-correlated single-photon counting (TCSPC) technique. As the excitation source we used a Ti:sapphire laser (Mai Tai BB, Spectra-Physics), which provides a repetition rate of 800 kHz with ~100 fs pulses generated by a home-made pulse-picker. The output pulse of the laser was frequency-doubled by a 1 mm thickness of a second harmonic crystal (β-barium borate, BBO, CASIX). The fluorescence was collected with a microchannel plate photomultiplier (MCP-PMT, Hamamatsu, R3809U-51) equipped with a thermoelectric cooler (Hamamatsu, C4878) connected to a TCSPC board (Becker & Hickel SPC-130). The overall instrumental response function was about 25 ps (the full-width at half-maximum (fwhm)). A vertically polarized pump pulse from a Glan-laser polarizer was used to irradiate samples and a sheet polarizer, set at an angle complementary to the magic angle (54.7°), was placed in the fluorescence collection path to obtain polarization-independent fluorescence decays.

XAFS measurements: The fluorescent XAFS measurements were performed at the Zn K-edge at BL-9A of the Photon Factory of the High Energy Accelerator Research Organization (KEK).[22] The 19-element SSD was used as the fluorescent detector. The sample solution was added to a brass cell sealed with Kapton windows and placed in a cryostat after freezing in liquid nitrogen. The EXAFS oscillations $c(k)$ given in Figure 37 of the Supporting Information were extracted by using the program REX2000 (Rigaku) to obtain the Fourier transforms given in Figure 38 of the Supporting Information. The area from 0.9–3.2 Å was Fourier-filtered to determine the bond distances for a fixed coordination number.

Acknowledgements

This work was supported by a Grant-in-Aid for Young Scientists (B, No. 19750122) and Scientific Research on Innovation Areas ("Coordination Programming" Area 2107, No. 22108533) from the Ministry of Education, Culture, Sports, Science, and Technology (MEXT) and the Ritsumeikan R-GIRO project (2008-2013). We thank Prof. Atsuhiro Osuka, Eiji Tsurumaki, and Taro Koide, Kyoto University, for X-ray analysis, Prof. Hiroshi Shinokubo and Dr. Satoru Hiroto, Nagoya University, for ESI-TOF MS, Prof. Tomohiro Miyatake, Ryukoku University, for FABMS, Prof. Yasuhiro Inada and Dr. Misaki Katayama, Ritsumeikan University, for XAFS (BL-9A at the Photon Factory), Dr. Sono Sasaki (at present, Kyoto Institute of Technology) and Dr. Hiroyasu Masunaga, JASRI/SPring-8, for synchrotron XRD analysis, and Prof. Hitoshi Tamiaki, Ritsumeikan University, for various measurements. T.H. thanks the JSPS for a Research Fellowship for Young Scientists and a Nishio Memorial Scholarship.

[1] For selected books on metal-assisted assemblies, see: a) *Transition Metals in Supramolecular Chemistry* (Ed.: J.-P. Sauvage), Wiley, New York, **1999**; b) *Metal-Containing and Metallosupramolecular Polymers and Materials* (Eds.: U. S. Schubert, G. R. Newkome, I. Manners),. ACS, Washington, **2006**.

[2] For recent reviews, see: a) D. Fiedler, D. H. Leung, R. G. Bergman, K. N. Raymond, *Acc. Chem. Res.* **2005**, *38*, 349–360; b) M. Shibasaki, M. Kanai, S. Matsunaga, N. Kumagai, *Acc. Chem. Res.* **2009**, *42*, 1117–1127.

[3] H.-J. Kim, D. Lee, H.-S. Park, M. Lee, *J. Am. Chem. Soc.* **2007**, *129*, 10994–10995.

[4] For recent reviews, see: a) J. R. Nitschke, *Acc. Chem. Res.* **2007**, *40*, 103–112; b) R. W. Saalfrank, H. Maid, A. Scheurer, *Angew. Chem.* **2008**, *120*, 8924–8956; *Angew. Chem. Int. Ed.* **2008**, *47*, 8794–8824.
[5] J. Xu, K. N. Raymond, *Angew. Chem.* **2006**, *118*, 6630–6635; *Angew. Chem. Int. Ed.* **2006**, *45*, 6480–6485.
[6] a) D. Schultz, F. Biaso, A. R. M. Shahi, M. Geoffroy, K. Rissanen, L. Gagliardi, C. J. Cramer, J. R. Nitschke, *Chem. Eur. J.* **2008**, *14*, 7180–7185; b) V. E. Campbell, X. de Hatten, N. Delsuc, B. Kauffmann, I. Huc, J. R. Nitschke, *Chem. Eur. J.* **2009**, *15*, 6138–6142.
[7] a) T. E. Wood, N. D. Dalgleish, E. D. Power, A. Thompson, X. Chen, Y. Okamoto, *J. Am. Chem. Soc.* **2005**, *127*, 5740–5741; b) J. M. C. Kerckhoffs, J. C. Peberdy, I. Meistermann, L. J. Childs, C. J. Isaac, C. R. Pearmund, V. Reudegger, S. Khalid, N. W. Alcock, M. J. Hannon, A. Rodger, *Dalton Trans.* **2007**, 734–742.
[8] For books and a review on dipyrrins, see: a) H. Fischer, H. Orth, *Die Chemie des Pyrrols, Vol. 2*, Akademische Verlagsgesellschaft, Leipzig, **1937**; b) H. Falk, *The Chemistry of Linear Oligopyrroles and Bile Pigments*, Springer, Vienna, **1989**; c) T. E. Wood, A. Thompson, *Chem. Rev.* **2007**, *107*, 1831–1861.
[9] For the synthesis of bidipyrrins, see: a) M. Bröring, *Synthesis* **2000**, 1291–1294; b) H. S. Gill, I. Finger, I. Božidarević, F. Szydlo, M. J. Scott, *New J. Chem.* **2005**, *29*, 68–71.
[10] For Zn^{II}-assisted double helices of bidipyrrins, see: a) Y. Zhang, A. Thompson, S. J. Rettig, D. Dolphin, *J. Am. Chem. Soc.* **1998**, *120*, 13537–13538; b) M. Bröring, S. Link, C. D. Brandt, E. C. Tejero, *Eur. J. Inorg. Chem.* **2007**, 1661–1670.
[11] a) M. Bröring, C. D. Brandt, J. Lex, H.-U. Humpf, J. Bley-Escrich, J.-P. Gisselbrecht, *Eur. J. Inorg. Chem.* **2001**, 2549–2556; b) M. Bröring, C. D. Brandt, J. Bley-Escrich, J.-P. Gisselbrecht, *Eur. J. Org. Chem.* **2002**, 910–917.
[12] a) The solid-state structure of **1a** is similar to the first example of an X-ray-analyzed *meso*-aryl-bidipyrrin Zn^{II} complex by Prof. Shinokubo (private communication); b) by X-ray diffraction (XRD) analysis, **1c** also showed solid-state lamella assemblies arising from van der Waals interactions between alkoxy units. As observed in the crystal structure of **1a**, the solid-state absorption spectrum suggests no notable interactions between the π moieties, Zn^{II}-assisted double helical parts, of **1c**.
[13] For metal coordination chemistry of phenylethynyl-bridged dimeric dipyrrins, see: a) H. Maeda, M. Hasegawa, T. Hashimoto, T. Kakimoto, S. Nishio, T. Nakanishi, *J. Am. Chem. Soc.* **2006**, *128*, 10024–10025; b) H. Maeda, T. Hashimoto, *Chem. Eur. J.* **2007**, *13*, 7900–7907.
[14] Gaussian 03, Revision D.02, M. J. Frisch, G. W. Trucks, H. B. Schlegel, G. E. Scuseria, M. A. Robb, J. R. Cheeseman, J. A. Montgomery, Jr., T. Vreven, K. N. Kudin, J. C. Burant, J. M. Millam, S. S. Iyengar, J. Tomasi, V. Barone, B. Mennucci, M. Cossi, G. Scalmani, N. Rega, G. A. Petersson, H. Nakatsuji, M. Hada, M. Ehara, K. Toyota, R. Fukuda, J. Hasegawa, M. Ishida, T. Nakajima, Y. Honda, O. Kitao, H. Nakai, M. Klene, X. Li, J. E. Knox, H. P. Hratchian, J. B. Cross, C. Adamo, J. Jaramillo, R. Gomperts, R. E. Stratmann, O. Yazyev, A. J. Austin, R. Cammi, C. Pomelli, J. W. Ochterski, P. Y. Ayala, K. Morokuma, G. A. Voth, P. Salvador, J. J. Dannenberg, V. G. Zakrzewski, S. Dapprich, A. D. Daniels, M. C. Strain, O. Farkas, D. K. Malick, A. D. Rabuck, K. Raghavachari, J. B. Foresman, J. V. Ortiz, Q. Cui, A. G. Baboul, S. Clifford, J. Cioslowski, B. B. Stefanov, G. Liu, A. Liashenko, P. Piskorz, I. Komaromi, R. L. Martin, D. J. Fox, T. Keith, M. A. Al-Laham, C. Y. Peng, A. Nanayakkara, M. Challacombe, P. M. W. Gill, B. Johnson, W. Chen, M. W. Wong, C. Gonzalez, J. A. Pople, Gaussian Inc., Wallingford CT, **2004**.
[15] For example, see: H. Katagiri, Y. Tanaka, Y. Furusho, E. Yashima, *Angew. Chem.* **2007**, *119*, 2487–2491; *Angew. Chem. Int. Ed.* **2007**, *46*, 2435–2439.
[16] CD changes that depend on guest-stimulated helical pitch stretching have recently been reported: K. Miwa, Y. Furusho, E. Yashima, *Nat. Chem.* **2010**, *2*, 444–449.
[17] F. Cheng, A. Adronov, *Chem. Eur. J.* **2006**, *12*, 5053–5059.
[18] C. B. Nielsen, J. Johnsen, J. Arnbjerg, M. Pittelknow, S. P. Mcllroy, P. R. Ogilby, M. Jorgensen, *J. Org. Chem.* **2005**, *70*, 7065–7079.
[19] CrystalStructure: Crystal Structure Analysis Package, Rigaku and Rigaku/MSC, The Woodlands, **2000**.
[20] SIR97: A program for crystal structure solution: A. Altomare, M. C. Burla, M. Camalli, G. L. Cascarano, C. Giacovazzo, A. Guagliardi, A. G. G. Moliterni, G. Polidori, R. Spagna, *J. Appl. Crystallogr.* **1999**, *32*, 115–119.
[21] SHELXL-97: Programs for Crystal Structure Analysis, G. M. Sheldrick, University of Göttingen (Germany), **1998**.
[22] M. Nomura, A. Koyama, *Nucl. Instrum. Methods Phys. Res. Sect. A* **2001**, *467–468*, 733–736.

Received: June 8, 2010
Published online: August 23, 2010

